IFAC SYMPOSIUM POWER SYSTEMS. MODELLING AND CONTROL APPLICATIONS

Brussels, 5-8 September 1988

DYNAMIC MODEL REDUCTION FOR THE MODAL ANALYSIS OF FREQUENCY AND POWER OSCILLATIONS IN LARGE POWER SYSTEMS

H. Weber, E. Welfonder
Department of Power Generation and Automatic Control, University of Stuttgart, Federal Republic of Germany

Abstract. In this paper a new method for the modal analysis of slow frequency and power oscillations - penetrating a whole electric power system - is presented.
By this Modal Power System Analysis Method there can not only be determined the damping degree and the period duration of the dominant power system oscillation, but also the location of those power plant units which are influencing the power system oscillations essentially.
Due to this fact also aimed counter actions can be derived. For being able to apply the Modal Power System Analysis Method also to large extended power systems an additional Dynamic Power System Reduction Method has been developed. By this method only those physical state variables inside of a considered subsystem are retained, which are essential for the dominant power system oscillation.
As an application case the northern part of the UCPTE-network has been chosen, where a strong power system oscillation had occured some years ago.

Keywords. Large electrical power systems, frequency and power oscillations, Modal Power System Analysis, Modal Power System Reduction, detection of instable power plants, stabilization measures.

INTRODUCTION

Between electrical part systems of large interconnected networks labile or even instable frequency and power oscillations can occur, if the relation between the installed power production capacity and the existing power transmission capacity is not balanced sufficiently (Heilemann, 1983).

Such lack of transmission capacity can be caused e.g. by normal line revision or by accidental line tripping after short circuits.

At present for the analysis of such phenomena the dynamic power system simulation method is mostly used, by which the stability or instability of a power system can be illustrated directly, but by which questions concerning the location and justification of damping equipments inside of a part system can be answered only by the trial-and-error-method (Fork, Clodius, Kaufhold, 1979).

This is due to the fact, that with the aid of simulation technique a deep insight into the dynamic behaviour of a part system is not possible; especially the question, which power plants are influencing the occured oscillations essentially, remains still unanswered.

Also analytical investigations concerning the power and frequency oscillations by calculating the resulting synchronizing and damping torque of every generator inside the part system are mostly too difficult because of the complexity of the real network.

Here the method of Modal Power System Analysis combined with Dynamic Power System Reduction offers an elegant new way for the investigation of electrical power systems.

With this method not only the dynamic input/-output behaviour of a part system seen from its coupling nodes can be analysed; but also the particular detection of those power plants is possible, which influence frequency and power oscillations essentially.

The information about the part system achieved that way can then be used for coordinated countermeasures, such as voltage controller justification as shown by Vournas, Papadias (1984), or location of power system stabilizers.

In real power systems the order of state variables however is normally too high for a direct application of the modal analysis method, therefore a stepwise performed dynamic reduction of the considered part system - retaining only the few essential state variables - has to be carried out before.

In this paper both methods, the Dynamic Power System Reduction and the Modal Power System Analysis, will be described.

CONSIDERED PART POWER SYSTEM

As practical application case the northern part of the UCPTE-network with the configuration in 1979 will be considered. In Fig. 1a the topology of the regarded part system, which is connected via two coupling lines of 150 km length to the center of the UCPTE-network, is shown. After a short circuit at the station DO 3 the lines marked with -//- were tripped off whereby the Subsystems I and II were switched off and isolated from the remaining UCPTE power system. Because of a power surplus in the isolated two Subsystem I and II the frequency increased to 50.25 Hz, whereas the frequency of the UCPTE-network remained at 50 Hz because of its size.

After the reconnection of the line Mo 3 - Do 3 the resynchronized power system became unstable, because of the loss of transmission capacity.

Figure 1d, (curve a) shows the simulated power oscillation on the line Mo 3 - Do 3. The oscillation period amounts to T_p = 2.93s, and the amplitude of the undamped oscillation increases continuously. This dangerous situation was stopped after switching off the voltage controllers in some power plants inside of the Subsystems I and II.

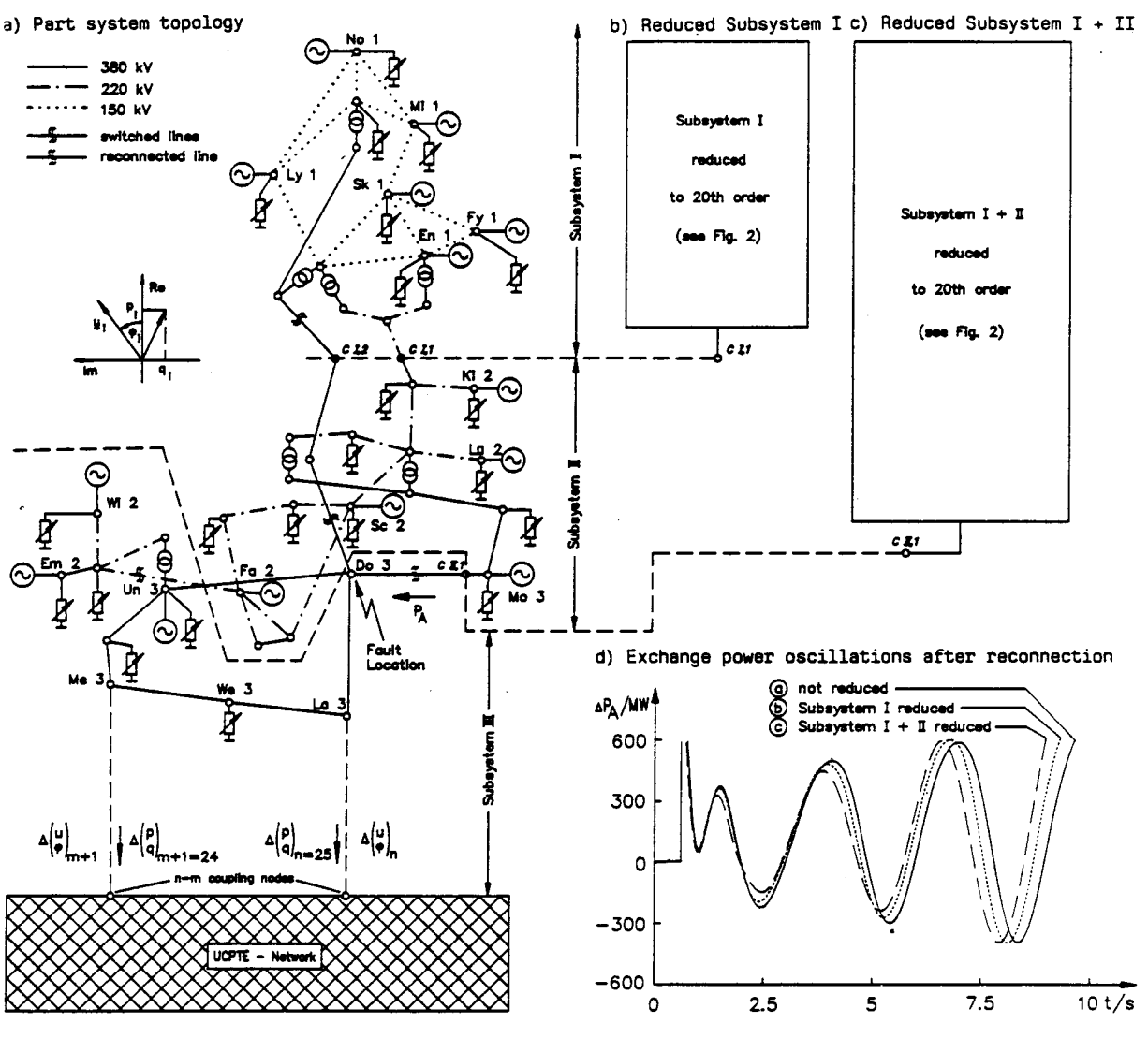

Fig. 1: Considered part system "North Part of UCPTE"

For the investigation of the occurred power system oscillation there could be based on the nonlinear dynamic power system model being developed by the authors for the detailed simulation of West European Power System (Welfonder, Schäfer, Asal, 1987).

Inside of this power system model all feed-in and feed-out nodes $\geq$ 100 MW are regarded individually by corresponding dynamic power plant and load models. Also inside of the power station the power plant units - feeding on different external nodes - are considered seperately.

As the modal analysis method is applicable only to linear systems the nonlinear dynamic model of the considered part power system in Fig. 1a has been linearized around its working point.

Subsequently the method of Dynamic Power System Reduction - described in the following - has been applied in two steps:

- at first only for the upper Subsystem I,s. Fig.1b and
- afterwards for the lower Subsystem II together with the already dynamically reduced Subsystem I, s. Fig. 1c.

A such stepwise performance turns out to be useful for limiting the dimension of the matrix equations and due to this also the computing time.

DYNAMIC POWER SYSTEM REDUCTION

The dynamic reduction of a part power system is possible, if the line flows to the neighbouring part systems remain unchanged after reduction also in the case of transient voltage fluctuations at the coupling nodes.

If this basic requirement can be fulfilled with sufficient accuracy in practice the nodes inside of the part system can be reduced totally and the dynamic state variables strongly.

Dynamic node reduction

The dynamic behaviour at a single node is caused by the active and reactive power-deviations of the producing power plant and/or the consuming load network:

$$\Delta \begin{pmatrix} P \\ q \end{pmatrix}_i = \underline{\underline{C}}_i \cdot \underline{x}_i + \underline{\underline{D}}_i \cdot \Delta \begin{pmatrix} u \\ \varphi \end{pmatrix}_i \qquad (1a)$$

Therein the state variables $\underline{x}_i = \begin{pmatrix} \underline{x}_P \\ \underline{x}_L \end{pmatrix}_i$
- of the power plant:

$$\underline{x}_{P_i} = \begin{pmatrix} \Delta\varphi_p \\ \Delta\omega_m \\ \Delta\psi_e \\ \Delta\psi_D \\ \Delta\psi_Q \\ x_{HD} \\ x_{ND} \\ x_Y \\ x_{SP} \\ x_e \\ x_f \\ x_{WO} \\ x_{PSS1} \\ x_{PSS2} \end{pmatrix}_i$$

rotor angle
angular velocity
flux linkage, exiter winding
flux linkage, d-axis damper winding
flux linkage, q-axis damper winding
high pressure turbine
low pressure turbine
steam valve servo
steam accumulator
field voltage
vco stabilization feedback
PSS-wash-out
PSS-lead-lag-element 1
PSS-lead-lag-element 2 (1b)

- and of the load network:

$$\underline{x}_{L_i} = \begin{pmatrix} x_f \\ x_u \\ \varphi \end{pmatrix}_i$$

frequency dependent power consumption
voltage dependent power consumption
voltage angle (1c)

can be computed at any time by the corresponding state differential equation:

$$\dot{\underline{x}}_i = \underline{\underline{A}}_i \cdot \underline{x}_i + \underline{\underline{B}}_i \cdot \Delta\left(\frac{u}{\varphi}\right)_i \qquad (1d)$$

Considering the dynamic behaviour of all nodes, it follows:

$$\underbrace{\Delta\begin{pmatrix} p_1 \\ q_1 \\ \vdots \\ p_m \\ q_m \end{pmatrix}}_{\Delta\left(\frac{p}{q}\right)_P} = \underbrace{\begin{pmatrix} \underline{\underline{C}}_1 & \cdots & \underline{\underline{0}} \\ \vdots & \ddots & \vdots \\ \underline{\underline{0}} & \cdots & \underline{\underline{C}}_m \end{pmatrix}}_{\underline{\underline{C}}_P} \cdot \underbrace{\begin{pmatrix} \underline{x}_1 \\ \vdots \\ \underline{x}_m \end{pmatrix}}_{\underline{x}_P} + \underbrace{\begin{pmatrix} \underline{\underline{D}}_1 & \cdots & \underline{\underline{0}} \\ \vdots & \ddots & \vdots \\ \underline{\underline{0}} & \cdots & \underline{\underline{D}}_m \end{pmatrix}}_{\underline{\underline{D}}_P} \cdot \Delta \underbrace{\begin{pmatrix} u_1 \\ \varphi_1 \\ \vdots \\ u_m \\ \varphi_m \end{pmatrix}}_{\Delta\left(\frac{u}{\varphi}\right)_P}$$

$$\Delta\left(\frac{p}{q}\right)_P = \underline{\underline{C}}_P \cdot \underline{x}_P + \underline{\underline{D}}_P \cdot \Delta\left(\frac{u}{\varphi}\right)_P \qquad (2a)$$

with

$$\underbrace{\begin{pmatrix} \dot{\underline{x}}_1 \\ \vdots \\ \dot{\underline{x}}_m \end{pmatrix}}_{\dot{\underline{x}}_P} = \underbrace{\begin{pmatrix} \underline{\underline{A}}_1 & \cdots & \underline{\underline{0}} \\ \vdots & \ddots & \vdots \\ \underline{\underline{0}} & \cdots & \underline{\underline{A}}_m \end{pmatrix}}_{\underline{\underline{A}}_P} \cdot \underbrace{\begin{pmatrix} \underline{x}_1 \\ \vdots \\ \underline{x}_m \end{pmatrix}}_{\underline{x}_P} + \underbrace{\begin{pmatrix} \underline{\underline{B}}_1 & \cdots & \underline{\underline{0}} \\ \vdots & \ddots & \vdots \\ \underline{\underline{0}} & \cdots & \underline{\underline{B}}_m \end{pmatrix}}_{\underline{\underline{B}}_P} \cdot \Delta \underbrace{\begin{pmatrix} u_1 \\ \varphi_1 \\ \vdots \\ u_m \\ \varphi_m \end{pmatrix}}_{\Delta\left(\frac{u}{\varphi}\right)_P}$$

$$\dot{\underline{x}}_P = \underline{\underline{A}}_P \cdot \underline{x}_P + \underline{\underline{B}}_P \cdot \Delta\left(\frac{u}{\varphi}\right)_P \qquad (2b)$$

The power flow between the different nodes can be derived from the load flow equations.
After linearisation around the working point the equations result:

- for the feed flows from the power plants or to the load networks (at the part system internal nodes) to:

$$\underbrace{\Delta\begin{pmatrix} p_1 \\ q_1 \\ \vdots \\ p_m \\ q_m \end{pmatrix}}_{\Delta\left(\frac{p}{q}\right)_P} = \underbrace{\begin{pmatrix} d_{1,1} & \cdots & d_{1,m} \\ \vdots & \ddots & \vdots \\ d_{m,1} & \cdots & d_{m,m} \end{pmatrix}}_{\underline{\underline{D}}_{PP}} \cdot \Delta \underbrace{\begin{pmatrix} u_1 \\ \varphi_1 \\ \vdots \\ u_m \\ \varphi_m \end{pmatrix}}_{\Delta\left(\frac{u}{\varphi}\right)_P} + \underbrace{\begin{pmatrix} d_{1,m+1} & \cdots & d_{1,n} \\ \vdots & \ddots & \vdots \\ d_{m,m+1} & \cdots & d_{m,n} \end{pmatrix}}_{\underline{\underline{D}}_{PC}} \cdot \Delta \underbrace{\begin{pmatrix} u_{m+1} \\ \varphi_{m+1} \\ \vdots \\ u_n \\ \varphi_n \end{pmatrix}}_{\Delta\left(\frac{u}{\varphi}\right)_C} \qquad (3a)$$

$$\Delta\left(\frac{p}{q}\right)_P = \underline{\underline{D}}_{PP} \cdot \Delta\left(\frac{u}{\varphi}\right)_P + \underline{\underline{D}}_{PC} \cdot \Delta\left(\frac{u}{\varphi}\right)_C$$

- and for the feed flows from or to the other part systems (at the external coupling nodes) to:

$$\underbrace{\Delta\begin{pmatrix} p_{m+1} \\ q_{m+1} \\ \vdots \\ p_n \\ q_n \end{pmatrix}}_{\Delta\left(\frac{p}{q}\right)_C} = \underbrace{\begin{pmatrix} d_{m+1,1} & \cdots & d_{m+1,m} \\ \vdots & \ddots & \vdots \\ d_{n,1} & \cdots & d_{n,m} \end{pmatrix}}_{\underline{\underline{D}}_{CP}} \cdot \Delta \underbrace{\begin{pmatrix} u_1 \\ \varphi_1 \\ \vdots \\ u_m \\ \varphi_m \end{pmatrix}}_{\Delta\left(\frac{u}{\varphi}\right)_P} + \underbrace{\begin{pmatrix} d_{m+1,m+1} & \cdots & d_{m+1,n} \\ \vdots & \ddots & \vdots \\ d_{n,m+1} & \cdots & d_{n,n} \end{pmatrix}}_{\underline{\underline{D}}_{CC}} \cdot \Delta \underbrace{\begin{pmatrix} u_{m+1} \\ \varphi_{m+1} \\ \vdots \\ u_n \\ \varphi_n \end{pmatrix}}_{\Delta\left(\frac{u}{\varphi}\right)_C} \qquad (3b)$$

$$\Delta\left(\frac{p}{q}\right)_C = \underline{\underline{D}}_{CP} \cdot \Delta\left(\frac{u}{\varphi}\right)_P + \underline{\underline{D}}_{CC} \cdot \Delta\left(\frac{u}{\varphi}\right)_C$$

By converting equations 3a to the internal voltage vector $\Delta(u\,\varphi)_P^T$ and by replacing the converted equation in equ. 3b the structure diagram, shown in Fig. 2a, will be obtained. This structure diagram already describes the active and reactive power flows at the coupling nodes in dependence of the coupling node voltages and in interaction with the power plant and load behaviour described by equ. 2.

The further conversion of equations 2 and 3 leads to the general structure diagram of Fig. 2b for the description of the part system input/output behaviour:

$$\Delta\left(\frac{p}{q}\right)_C = \underline{\underline{C}} \cdot \underline{x} + \underline{\underline{D}} \cdot \Delta\left(\frac{u}{\varphi}\right)_C \qquad (4a)$$

with the belonging state equation

$$\dot{\underline{x}} = \underline{\underline{A}} \cdot \underline{x} + \underline{\underline{B}} \cdot \Delta\left(\frac{u}{\varphi}\right)_C \qquad (4b)$$

By this deduction all nodes inside of the part system have been eliminated; however all internal state variables, describing the dynamics of the part system, remain active unreduced further on.

Dynamic State Reduction

From the great number of state variables being active inside of the part system only a few are influencing the dynamic behaviour at the coupling nodes essentially. Therefore a dynamic state reduction seems possible and necessary too for the stepwise reduction of big part systems to be modal analysed.

For this purpose the derived state equation (4) - generally describing the input/output behaviour of the part system at the coupling nodes - has in the first stage to be transformed by

$$\underline{x} = \underline{\underline{V}} \cdot \underline{z} \qquad (5a)$$

in the modal state domain (Föllinger, 1972):

$$\Delta\left(\frac{p}{q}\right)_C = \underbrace{\underline{\underline{C}} \cdot \underline{\underline{V}}}_{\hat{\underline{\underline{C}}}} \cdot \underline{z} + \underline{\underline{D}} \cdot \Delta\left(\frac{u}{\varphi}\right)_C$$

$$\Delta\left(\frac{p}{q}\right)_C = \hat{\underline{\underline{C}}} \cdot \underline{z} + \underline{\underline{D}} \cdot \Delta\left(\frac{u}{\varphi}\right)_C \qquad (5b)$$

with

$$\dot{\underline{z}} = \underbrace{\underline{\underline{V}}^{-1} \cdot \underline{\underline{A}} \cdot \underline{\underline{V}}}_{\underline{\underline{\Lambda}}} \cdot \underline{z} + \underbrace{\underline{\underline{V}}^{-1} \cdot \underline{\underline{B}}}_{\hat{\underline{\underline{B}}}} \cdot \Delta\left(\frac{u}{\varphi}\right)_C$$

$$\dot{\underline{z}} = \underline{\underline{\Lambda}} \cdot \underline{z} + \hat{\underline{\underline{B}}} \cdot \Delta\left(\frac{u}{\varphi}\right)_C \qquad (5c)$$

where the eigenvalues of the part system are written explicitely in the main diagonal of the transformed system matrix, $\underline{\underline{\Lambda}}$ s. Fig. 2c.

The advantage of this modal state description is that the eigenvalues $\underline{\lambda}_k = \delta_k + j\omega_k$ are specifying the swinging and damping behaviour of the eigenmovements totally being active inside of the part system; so e.g. a eigenvalue with $\delta_k = 0$ characterizes an undamped power system oscillation, details see below.

In the second stage the eigenvariables are devided into dominant ones and non dominant ones. This is done with the aid of the domincance measure from Litz (1980):

$$S_k = \sum_{i,j} \left| \frac{\hat{\underline{D}}_{kj} \cdot \hat{\underline{C}}_{ik}}{\underline{\lambda}_k} \right| \qquad (6a)$$

which describes for each eigenvariable $\underline{z}_k$ the summed up influence from all coupling node voltages $\Delta(u\,\varphi)_C^T$ to all tieline flows $\Delta(P\,Q)_C^T$ and this referred to the eigenvalue $\underline{\lambda}_k$.

In the following the evaluation of the dominant eigenvariables is pointed out for the example of Subsystem I, illustrated in Fig. 1a, which consists unreduced of 105 state variables.

In Fig. 3 the eigenvalues with the 13 greatest dominance measures are arrangead in decreasing sequence of the dominance measures.

As to be seen from this figure only the first 15 eigenvalues contain a considerable domincance measure of > 1 % related to the highest value. Therefore the regarding of the corresponding 15 eigenvariables would have been sufficient. In fact 20 eigenvariables $\underline{z}_d$ have been chosen as dominant, because all part systems which have been considered could be reduced down to this number independent of the order of the unreduced part system.

a) physical structure

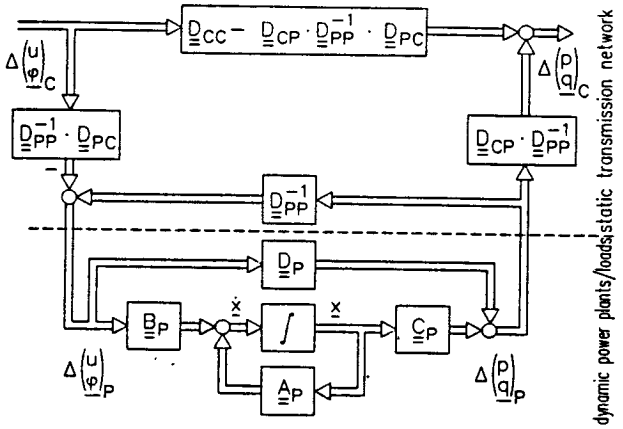

b) node reduced structure

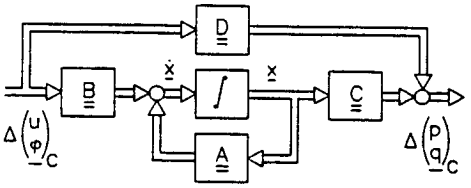

c) modal transformed structure with dominance detection

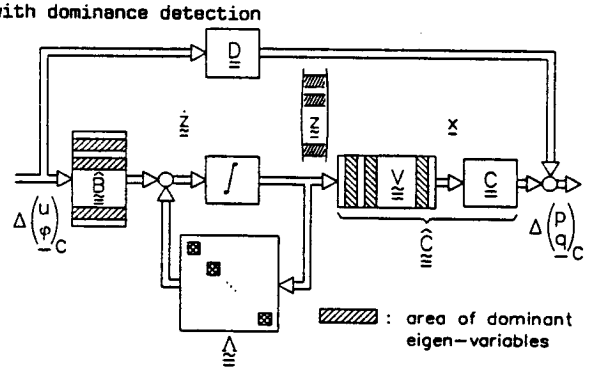

d) modal structure, devided in dominant and non dominant eigenvariables

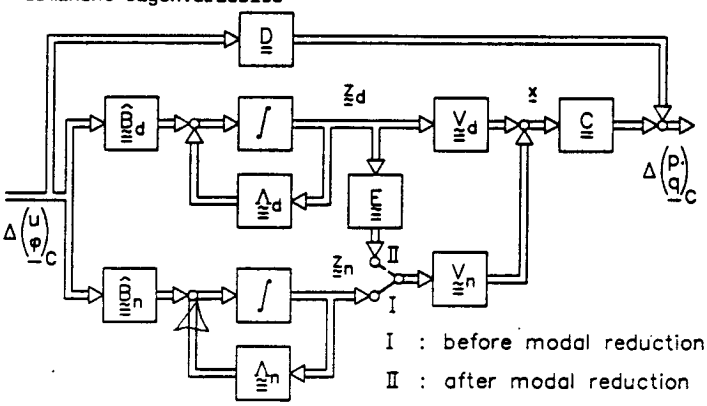

In the third stage the remaining eigenvariables being identified as non-dominant are replaced by an equivalent linear combination of the dominant eigenvariables $\underset{\sim}{z}_d$. This leads to the reduced transformation matrix:

$$\underset{\sim}{V}^{*}_{d} = \underset{\sim}{V}_{d} + \underset{\sim}{E} \cdot \underset{\sim}{V}_{n}$$

wherein the correction matrix $\underset{\sim}{E}$ will be determined in such a way that the averaged square error of:

$$\underset{\sim}{\varepsilon}_d = \underset{\sim}{z}_n - \underset{\sim}{E} \cdot \underset{\sim}{z}_d$$

goes to minimum.

e) modal reduced structure

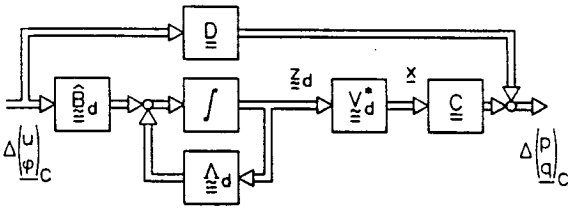

f) modal reduced structure, devided in essential and unessential state variables

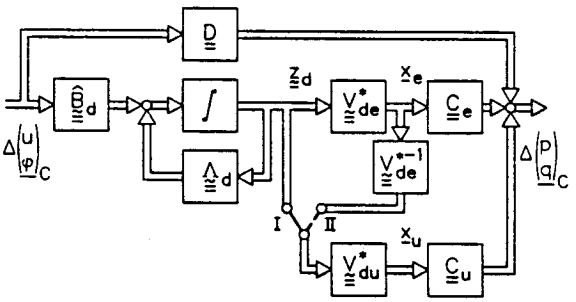

g) modal and state reduced structure

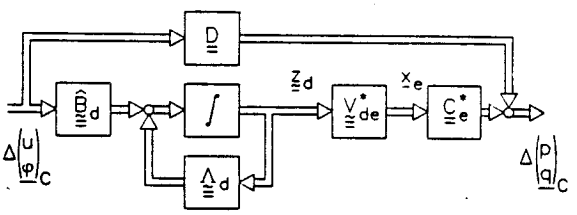

h) retransformed reduced structure

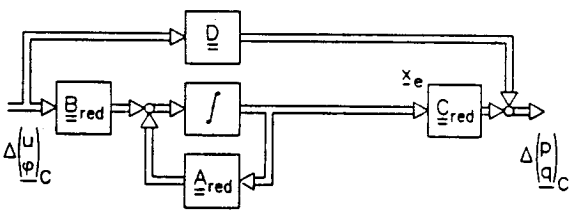

Fig.2: Node- and modal-state-reduction of an electrical part system

Reduction of the state variables

Up to now only the eigenvariables $\underset{\sim}{z}$ have been reduced but not the great number of the physical state variables $\underset{\sim}{x}$.

To achieve this the state variable have also to be divided into essential and unessential ones and this separately for each eigenvariables $\underset{\sim}{z}_k$. This can be done by means of an additional "essential measure" developed by Barth, Jaschek (1985):

$$Q_{mk} = \left| \sum_j \frac{\underset{\sim}{v}_{mk} \cdot \hat{\underset{\sim}{b}}_{kj}}{\underset{\sim}{\lambda}_k} \right| \qquad (6b)$$

which describes for each eigenvariables $\underset{\sim}{z}_k$ the summed up influence from all coupling node voltages $\Delta(u\,\varphi)_C$ to each state variable x_m refering to the eigenvalue $\underset{\sim}{\lambda}_k$.

Using the essential measure the evaluation of the main state variables can be carried out in the same manner as the described determination of the dominant eigenvariables.

When choosing the number of essential state variables $\underline{x}_e$ equal to the order of the dominant eigenvariables $\underline{z}_d$, the remaining essential part of the transformation matrix $\underline{V}^*_{de}$ becomes quadratic and can be inverted too.

In this case the unessential state variables can be eleminated by reducing the output matrix $\underline{C}$ to

$$\underline{C}^*_e = \underline{C}_e + \underline{C}_u \cdot \underline{V}^*_{du} \cdot \underline{V}^{*-1}_{de} \qquad (7)$$

Using $\underline{V}^*_{de}$ as reduced transformation matrix the modal transformed and reduced part system can also be retransformed in the physical model structure again.

Stepwise Reduction of large Part Systems

The described method for "Dynamic Power System Reduction" shall now be applied to the northern part of the UCPTE-network. Therefore the Part System is divided in three Subsystems I - III, as marked in Fig. 1a.

In the first step Subsystem I is reduced:
- external to the coupling node CI,1 and
- internal from 105th order to 20th order, s. Fig. 1b

In the second step Subsystem II and the reduced Subsystem I are reduced together:
- external to the coupling node CII,1 and
- internal from 117th again to 20th order, s. Fig. 1c

In Fig. 1d there is illustrated the simulated exchange power flow between the nodes Mo 3 - Do 3 when reconnecting the two Subsystem I and II with Subsystem III and due to this with the remaining large UCPTE network.Therein the simulation has been carried out for:

a) the unreduced Subsystems I - III,
total order: n = 262

b) the only reduced Subsystem I, Subsystems II and III unreduced
total order: n = 177

c) the reduced Subsystems I and II, Subsystem III unreduced
total order: n = 80

As it can be seen in Fig. 1d the correspondance of the simulated exchange power flows is very well. Period duration and damping degree of the increasing power oscillation are retained nearly equal, also after a reduction of the eigen-/and state variables from 262 to 80, that means down to 30 %.

Number	Eigenvalues / $\frac{1}{s}$	Dominance Measures (0 20 40)
1,1'	−0,33 ± j· 3,69	
2,2'	−4,63 ± j· 4,26	
3,3'	−4,50 ± j·11,30	
4	−14,6	
5,5'	−7,67 ± j· 2,61	
6	−34,30	
7	−5,52	
8	−3,83	
9	−29,80	
10,10'	−4,62 ± j· 9,56	
11,11'	−3,63 ± j· 7,61	
12	−3,12	
13,13'	−0,70 ± j· 0,004	

Fig. 3: First thirteen eigenvalues of Subsystem I with greatest dominance measures

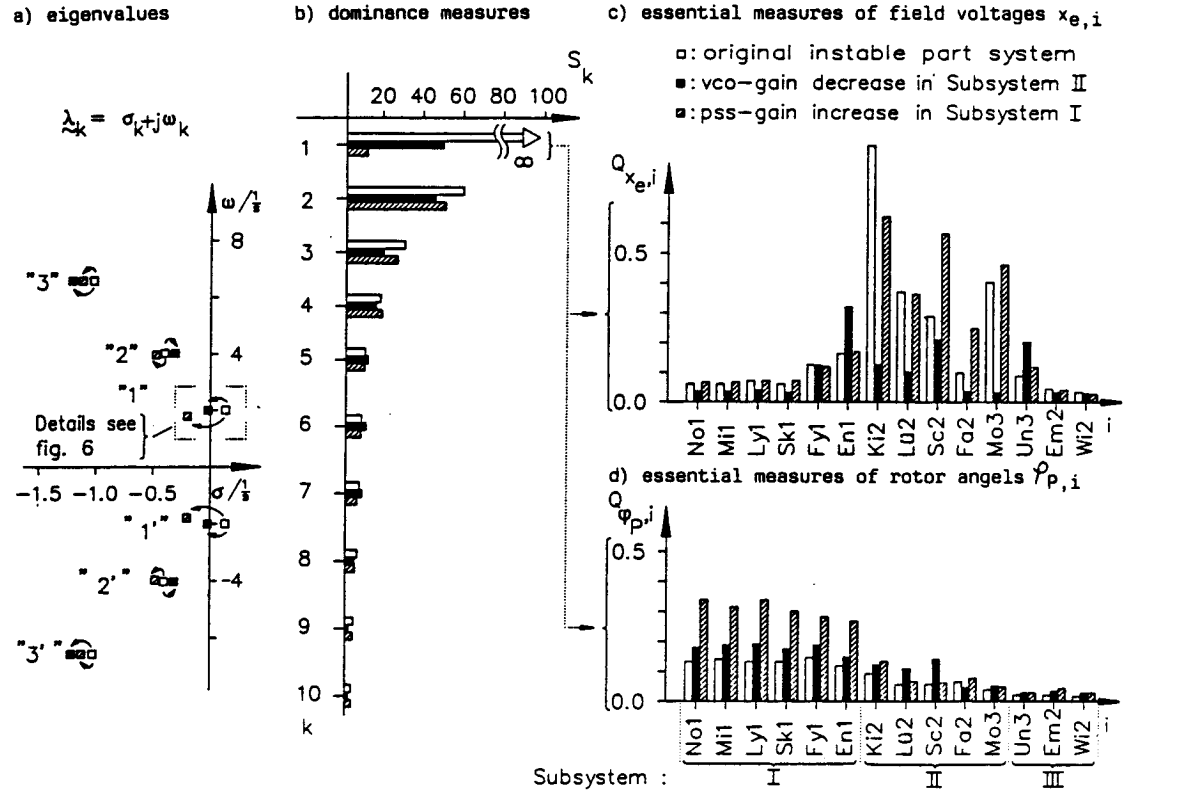

Figure 4: Eigenvalues, dominance measures and essential measures of the part system with ▬ ▨ and without ▭ damping actions

MODAL POWER SYSTEM ANALYSIS

The dynamic reduction of the considered northern part of the UCPTE-network has been carried out in such a way, that there has been retained:

- the coupling node C II,1 between Subsystem II and III,
- the 20 most dominant eigenvariables and
- the 20 most essential state variables of the reduced Subsystem I and II.

This reduced Part System has now - in connection with the big UCPTE-networks - to be modal analysed. The results aimed by this analysis are summarised and white marked in Fig. 4:

For the first three dominant eigenvariables, to be seen in Fig. 4b the belonging eigenvalues are illustrated in Fig. 4a. In Fig. 4c and d there are shown in addition for the most dominant instable-eigenvalues the essential measures of the field voltages x_e as well as of the corresponding rotor angles γ_p.

As to be seen:

- the oscillation - belonging to the first eigenvalue $\underset{\sim}{\lambda}_{1,1'} = (0.14 \pm j2.28)$ 1/s is instable, increasing with a period duration of $T_{p1} = (2\pi/2.28)$ s = 2.76 s.
  This part system oscillation is caused by the coherent swinging of the three Subsystems I - III against the big UCPTE-network, as illustrated in Fig. 5b
- the second oscillation - belonging to $\underset{\sim}{\lambda}_{2,2'} = (-0.4 \pm j4.27)$ 1/s is already strongly damped, decreasing with a period duration of $T_{p2} = (2\pi/4.27)$ s = 1.47 s.
  This oscillation is caused by the coherent swinging of the two Subsystems I and II against Subsystem III, as shown in Fig. 5c
- the third oscillation - belonging to $\underset{\sim}{\lambda}_{3,3'} = (-1.08 + j6.7)$ 1/s is very strongly damped, decreasing with a period duration of $T_{p3} = (2\pi/6.7)$ 1/s = 0.94 s.
  This third oscillation is related to the swinging of all Subsystems against each other, as illustrated in Fig. 5d.

Therein Fig. 5 shows a mechanical analogon consisting of three damped balls and three coupling rods, representing the three Subsystems which are operating against the big UCPTE-network.

a) four-balls three-rods swinging model with damping

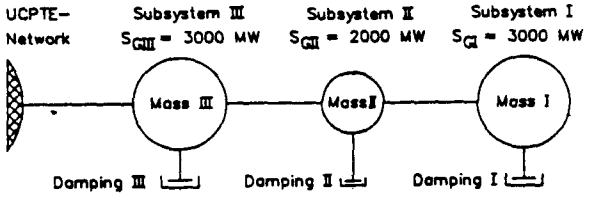

b) movement corresponding with eigenvalue 1,1'

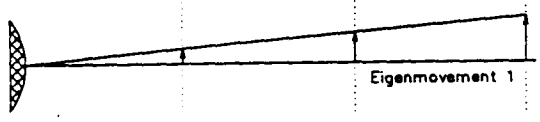

c) movement corresponding with eigenvalue 2,2'

d) movement corresponding with eigenvalue 3,3'

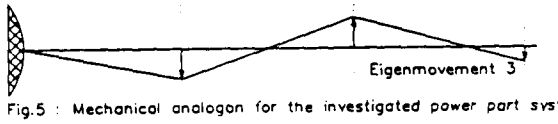

Fig.5 : Mechanical analogon for the investigated power part system

STABILIZING COUNTER ACTIONS DERIVED BY MODAL ANALYSIS

Considering Fig. 4c and d in detail one recognizes, that the field voltage $x_{e\ Ki2}$ has the greatest essential measure.

Therefore at first the voltage controller gain of this generator has been decreased strongly from about 250 to 10 pu. However this counter action alone has been not sufficient for stabilizing the power system oscillation, see Fig. 6, countermeasure IV. Therefore in addition all voltage controller gains in Subsystem II - having also great essential measures - have been decreased to 10 pu. This results already to a stable eigenvalue behaviour, but with only rather small damping, see Fig. 6, countermeasure II. Thereby the belonging eigenvalues, dominance measures and essential measures are shifted as shown black marked in Fig. 4.

Decreasing the voltage controller gains of Subsystem I instead of Subsystem II leads to no essential improvement, see the furtheron instable behaviour in Fig. 6, alternative countermeasure V. The reason is, that the field voltages of the generators inside of Subsystem I have only small essential measures.

Inside of Subsystem I however the rotor angles γ_p have significant essential measures. Therefore an installation of stabilizers at the belonging generators leads to a stable behaviour with a already sufficient damping, see alternative countermeasure III in Fig. 6.

The corresponding movement of the eigenvalues, dominance measures and especially of the essential measures is illustrated hatched marked in Fig. 4 too.

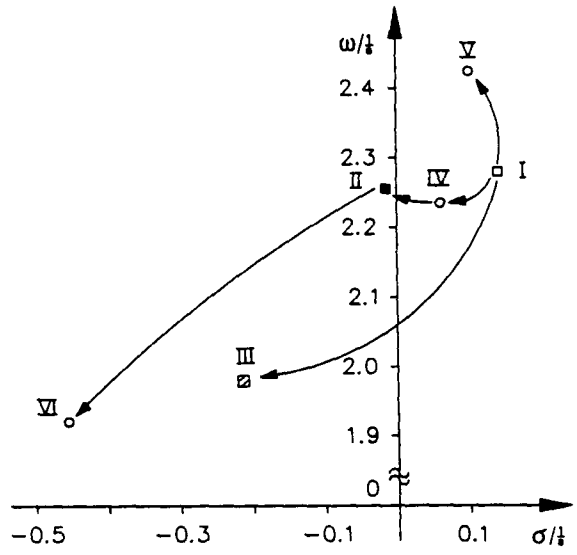

without counter measures

I : original instable part system

considered counter measures

II : vco-gain decrease in Subsystem II

III : pss-gain increase in Subsystem I

IV : vco-gain decrease only in power plant Ki 2

V : vco-gain decrease in Subsystem I

VI : vco-gain decrease in Subsystem II and pss-gain increase in Subsystem I

Fig. 6: Movement of the instable eigenvalue 1 for different stabilization measures

When applying both stabilizing countermeasures II and III in addition i.e. decreasing the voltage controller gains in Subsystem II and installing power system stabilizers in Subsystem I the considered part system will be stabilized very strongly, see Fig. 6 countermeasure VI.

The efficiency of the stabilizing counter measure actions II, III and VI is finally illustrated in Fig. 7 by the simulated exchange power flow occurring after the reconnection of the Subsystem I and II (and this in comparison to the original instable behaviour without any counter action).

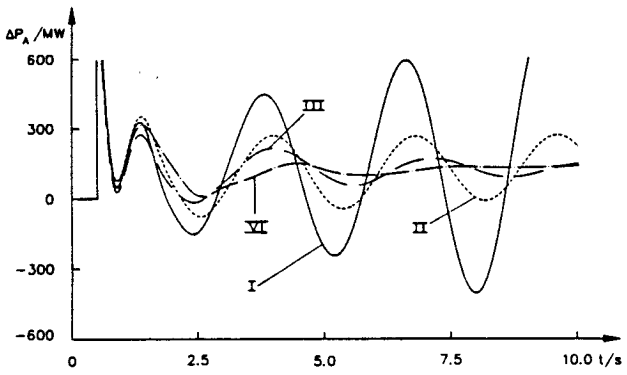

Fig. 7: Exchange power flow Mo3-Do3 with and without stabilizing measures

CONCLUSION

In this paper there has been described on the one hand a method for Dynamic Power System Reduction, retaining only:

- the coupling nodes
- the most dominant eigenvariables and
- the essential physical state variables

of a considered subsystem. This method can also be applied stepwise to several subsystems.

On the other hand a method for Modal Power System Analysis has been presented, by which can be determined:

- the damping degrees and the period durations of the dominant oscillation inside of a considered power system,
- the locations of the power plant units and their control loops influencing the dominant power system oscillations essentially,
- aimed counter measures.

Both methods have been applied to the north part of the UCPTE-network. Therein could be shown by modal analysis that the considered Part System could be stabilized - after reconnecting to the UCPTE-power system - by decreasing the voltage controller gains of the generators in Subsystem II or/and by installing appropriate power system stabilizer in Subsystem I.

REFERENCES

Barth, J.; Jaschek, H. (1985) Ermittlung wesentlicher Zustandsgrößen bei der modalen Ordnungsreduktion . Automatisierungstechnik, 7/85, S. 219-226.

Föllinger, O.; u.a. (1972) Regelungstechnik. Elitera-Verlag Berlin, 1972. ISBN 3-7785-02395.

Fork, K.; Clodius, D.; Kaufhold, W. (1979) Einfluß der Spannungs- und Turbinenregelung auf das dynamische Verhalten großer Dampfturbosätze am Netz. ETG Fachtagung 5, Berlin, 1979

Heilemann, F. (1983) Frequenz- und Leistungspendelungen in elektrischen Verbundnetzen, Entstehung und Gegenmaßnahmen. Dissertation Universität Stuttgart

Heilemann, F.; Welfonder, E. (1983) Investigation of Low Frequency and Power Oscillations Appearing in Large Extended Power Systems. CIGRE IFAC Symposium, Florenz.

Litz, L. (1980) Order reduction of linear State-Space models via optimal approximation of the nondominant modes. IFAC Symposium, Toulouse.

Vournas, C.D.; Papadias, B.C. (1984) Excitation control schemes in the hellenic interconnected system for the improvement of system dynamic performance. CIGRE 84, 39-05.

Welfonder, E.; Schäfer, S.; Asal, H.P. (1987) Control Behaviour of the West European Power System Simulated on the Basis of a Detailed Dynamic Model. 10th IFAC World Congress, Munich.